TUDelft

Delft University of Technology

Comfort and Time Efficiency
A Roundabout Case Study

Zheng, Yanggu ; Shyrokau, Barys; Keviczky, Tamas

Comfort and Time Efficiency: A Roundabout Case Study

Yanggu Zheng[1], Barys Shyrokau[1] and Tamas Keviczky[2]

Abstract— The public acceptance of automated driving is influenced by multiple factors. Apart from safety being of top priority, comfort and time efficiency also have an impact on the popularity of automated vehicles. These two factors contradict each other as optimizing for one results in the degradation of the other. We investigate in this paper how such a multi-objective problem is approached by human drivers and by numerical optimization in the roundabout scenario, which is compact in size but complex to handle. The human drivers' behavior is first observed using naturalistic driving data. The average trajectories and distribution of peak accelerations were extracted after model-based fitting and removal of erroneous samples. The processed data is shared online as an open-access dataset. Then, an optimization problem is formulated and solved to find the numerically optimal motion profile in terms of comfort and time efficiency. The weighted sum of travel time and discomfort is minimized. By adjusting the weight distribution, we present different motion profiles favoring optimal comfort, human-like acceleration magnitudes, and agility, respectively.

I. Introduction

The research interest in automated driving has been constantly growing, thanks to the potential societal benefits it promises to bring about. Apart from reducing road fatalities due to human errors, the considerable amount of time saved from performing the driving task on a regular basis is also beneficial. To efficiently utilize such time, automated vehicles should further improve their comfort level, as physical discomfort and motion sickness may harm the occupants' performance in cognitive tasks [1]. A major contributing factor to discomfort and motion sickness is the translational accelerations [2][3]. Longitudinal and lateral accelerations can be reduced by changing speed gently and negotiating the corners at a lower speed. A survey suggests that around 10% of the passengers often or almost always experience carsickness [4]. If they were to become the users of automated vehicles, the motion planner should focus on optimizing the comfort level. Prior to automated vehicles, this topic was covered under the motion planning studies on wheeled robots with non-holonomic kinematics. The relevant studies primarily focus on the smoothness of the planned path, where the continuity of curvature and its derivatives are of interest. The field has seen the development of methods based on Dubins' curves, clothoids, etc. [5]. The smooth curves are considered suitable for comfort in a qualitative manner

[6]. However, driving on public roads is a more complex and dynamic task, further requiring the vehicle to adopt a proper velocity on top of a safe and smooth spatial path. Moreover, motion comfort is a more comprehensive quality to measure than the smoothness of a curve. Hence, comfort-oriented motion planning has received some research interest in recent years. For sake of simplicity, some studies opt for decoupled approaches and focus on longitudinal motion only. Again, smooth curve classes have been exploited to improve comfort. Lattarulo et al. [7] defined the velocity profile with quintic Bezier curves and Du et al. [8] chose the hyperbolic tangent function for a similar purpose. Some other studies quantitatively optimize longitudinal motion comfort by minimizing a cost function related to jerk [9][10][11]. The other way of decoupling the motion planning problem is to assume a constant velocity and plan the path for specific use cases. These studies mainly exploit similar techniques as in smooth path planning, using parametric curves [12] or motion primitives [13]. Combined path and velocity planning for comfort is less addressed due to the complexity of the problem. Shin et al. [14] proposed a comfort planner for car-like robots to avoid obstacles with a minimal integral of acceleration and travel time. Htike et al. [15] adopted a similar idea although the motion sickness dose value (MSDV) is used as the comfort measure instead.

Optimizing comfort could come at the cost of a longer travel time, which is frustrating for the passengers who are less susceptible to motion sickness or on an urgent trip. As in [14] and [15], travel time should also be considered when evaluating the planned motion. Solving this multi-objective optimization problem helps reveal the full potential that automated vehicles can achieve. The optimal solution set allows the motion planner to adapt to user preferences within a safe and feasible range. The user is able to choose between a higher comfort level or a swifter ride. The choice could be less intuitive for inexperienced users though. Thus a default setting that results in a human-like motion is helpful. The naturalistic driving trajectories of human drivers can be exploited to help describe the average human driving behavior.

Various scenarios have been adopted in the literature to demonstrate the performance of the motion planning algorithms. The naturalistic driving data also covers highly diverse driving situations. In order to make an efficient comparison between human drivers and motion planners, a common, compact, and nonetheless complex scenario is needed. The roundabout scenario meets these requirements as it demands properly adjusted speed and path from the passing vehicles while involving moderate maneuvering ef-

[1]Yanggu Zheng and Barys Shyrokau are with the Department of Cognitive Robotics, Faculty of Mechanical, Maritime & Materials Engineering, Delft University of Technology, 2628 CD Delft, The Netherlands `y.zheng-2@tudelft.nl`, `b.shyrokau@tudelft.nl`

[2]Tamas Keviczky is with Delft Center for Systems and Control, Faculty of Mechanical, Maritime & Materials Engineering, Delft University of Technology, 2628 CD Delft, The Netherlands `t.keviczky@tudelft.nl`

fort. This scenario has been adopted in studies on various topics related to automated driving [16][17].

In this paper, we investigate how the conflict of interest between comfort and time efficiency can be approached, and concentrate the effort on the roundabout scenario. First, the naturalistic driving data from the ACFR dataset [18] is utilized to understand the comfort level of average human drivers. Then, an optimization problem is formulated where the weighted sum of discomfort and travel time for navigating through a roundabout should be minimized. The weighting between the two factors can be exploited to adapt to the user's preference. On one side, the comfort-optimal motion profiles are obtained, which benefit passengers who are highly susceptible to motion sickness. The motion profiles reflecting human-like acceleration levels are then determined for the default weighting. Towards the other end, we also present more aggressive motion profiles for urgent trips.

The rest of the paper is structured as follows. Section II focuses on processing the naturalistic driving data. The detailed formulation of the optimization problem for maneuvering at a roundabout is given in Section III. The results from the two sections are presented in Section IV, where we first show the human drivers' behavior at roundabouts and then present the optimized motion profiles. The work is concluded in Section V where we discuss the findings and limitations of this study and point out potential future opportunities.

II. HUMAN PERFORMANCE BASELINE

As the first step of this study, we aim to observe and characterize human driving behavior at roundabouts from naturalistic driving data. The ACFR dataset is chosen as it contains over 23,000 runs recorded at five roundabouts on public roads. The traffic vehicles were tracked primarily using LiDAR, which is installed on top of the data collection vehicle parked close to the intersection. The position of a traffic vehicle is estimated with the center of its bounding box. The generation of bounding boxes is sensitive to the shape of the recorded vehicle and occasionally suffers from occlusions. Hence, the time-stamped position data is rather noisy and is not suitable for extracting the velocity directly, nor for finding the higher-order derivatives which have more impact on comfort. Furthermore, the dataset contains erroneous recordings that are not representative of driving a passenger vehicle. Additional processing effort has been involved to overcome these issues. These tasks are described in the following subsections.

A. Trajectory Reconstruction

To handle the measurement noise and errors, an optimization-based trajectory reconstruction has been performed. The motion profiles are reconstructed based on the point-mass kinematics (1) to ensure feasibility and continuity. The motion of the vehicle is described by x, y, velocity v, and heading angle ψ. The motion is controlled by the longitudinal acceleration $\dot{v}$ and angular acceleration $\ddot{\psi}_i$. The equations of motion are integrated with an Euler step of t_s, the sampling time of the original data. The motion
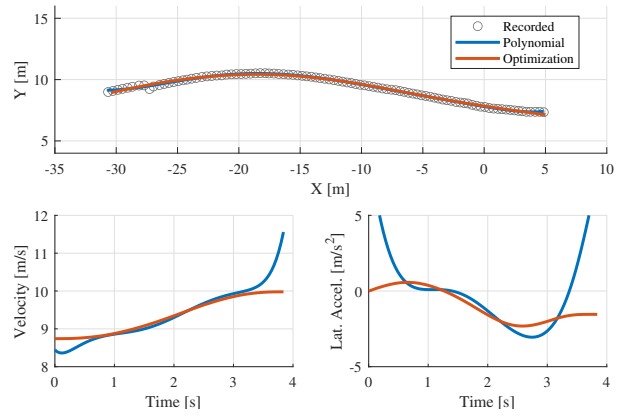

Fig. 1. An example of the reconstructed trajectory by the optimization-based method in comparison to polynomial fitting.

profile obtained from an input sequence is evaluated with a cost function in the form of (2) that penalizes the spatial deviation from the measured positions added to the input effort involved.

$$
\begin{aligned}
x_{i+1} &= x_i + v_i \cos \psi_i \cdot t_s \\
y_{i+1} &= y_i + v_i \sin \psi_i \cdot t_s \\
v_{i+1} &= v_i + \dot{v}_i \cdot t_s \\
\dot{\psi}_{i+1} &= \dot{\psi}_i + \ddot{\psi}_i \cdot t_s \\
\psi_{i+1} &= \psi_i + \dot{\psi}_i \cdot t_s
\end{aligned}
\tag{1}
$$

$$
J_1 = \sum_{i=1}^{N} \left(\varepsilon_i^T Q \varepsilon_i + u_i^T R u_i \right)
$$
$$
\varepsilon_i = \begin{bmatrix} x_i \\ y_i \end{bmatrix}_{\text{rec}} - \begin{bmatrix} x_i \\ y_i \end{bmatrix}_{\text{est}}, u_i = \begin{bmatrix} \dot{v}_i \\ \ddot{\psi}_i \end{bmatrix}
\tag{2}
$$

By minimizing this cost function, an optimal reconstruction of the recorded trajectory could be achieved. The total processing time of the entire dataset is approximately 3 days on a desktop PC (Intel Xeon W-2145 CPU). A 7th order polynomial fitting method was implemented as an alternative approach, in order to demonstrate the benefits of incorporating basic kinematics and penalizing the input effort. Each trajectory is described with the x- and y-coordinates versus time and the two sequences are fitted into two corresponding polynomials. The comparison between the two methods is given in Fig. 1, performed on a random recording in the dataset. It is evident that the original data is of poor quality. A strong discontinuity can be found on the left-hand side of the recorded trajectory. Both methods are able to reconstruct a smooth spatial path. However, the velocity and acceleration profiles from the polynomial method are less feasible because it solely minimizes the fitting error. The optimization-based method reflects a more reasonable driving behavior in contrast.

B. Outlier Removal

As mentioned above, the dataset contains an unknown amount of erroneous recordings that are not representative of driving a passenger vehicle. To exclude these samples, we adopt the DBSCAN (density-based spatial clustering of applications with noise) algorithm that is widely used in data science. Essentially, the algorithm clusters the samples according to a distance metric (e.g., the Euclidean distance). In each iteration, a new cluster starts with a random sample that does not yet belong to any existing cluster. The cluster grows by repetitively including the nearby samples whose distance to existing samples in the cluster is below a certain threshold. The reconstructed trajectories are first interpolated to an equal number of steps so that the dimensions match. The trajectories recorded at the same location and having identical entry-exit combinations are grouped together and DBSCAN is performed separately on each group. The samples belonging to the largest cluster are considered the most representative and the rest are discarded. We used the standard implementation of DBSCAN in MATLAB, where the critical parameter is the distance metric. Ideally, the parameter is tuned to distinguish between erroneous samples and the samples that are only different so that the diversity in the accepted samples is still preserved. We adapt this parameter to different types of maneuvers, considering that a longer maneuver would naturally have a larger variance between drivers. Although it is infeasible to manually check all the samples, we present in Fig. 2 a random example of a rejected recording in comparison to an accepted one. The rejected recording indeed exhibits a different behavior as the object had a significantly lower speed towards the end and departed from the drive lane after the roundabout. This could be, e.g., a cyclist mistakenly classified as a motor vehicle, diverting to the sidewalk. Fig. 3 shows the variance of the data before and after removing the outliers. The points on the 2-D plane represent the coefficient of the first and second principal components (PC1 and PC2, respectively) determined by the principal component analysis (PCA). The high-ranking principal components are the projected directions in which the samples have a larger variance. Thus PCA highlights the data variation in a compact manner and also simplifies the visualization. The results suggest a better concentration of data after the outliers are removed. The processed and validated recordings are collected in a dataset that is open-access via IEEE DataPort[1].

III. Optimal Maneuver at a Roundabout

In this section, we formulate an optimization problem to find the optimal motion profile at roundabouts. The optimality of the motion is characterized by comfort and time efficiency. The optimization is performed for three typical maneuvers: turning right, driving straight (i.e. taking the exit with the same heading), and turning left. These match the maneuvers from the naturalistic driving data, although
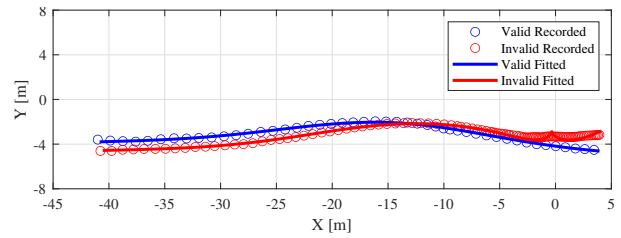
Fig. 2. Comparison between an acceptable sample and a sample deemed invalid by DBSCAN.
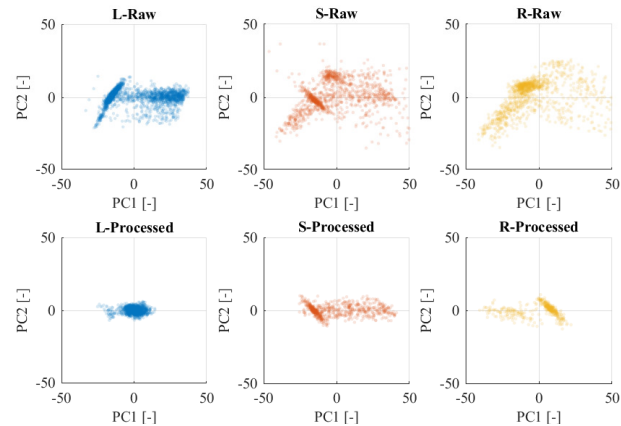

Fig. 3. A compact visualization of data variance with PCA before (upper row) and after (lower row) removing the outliers.

the latter is for left-handed traffic, and hence the left- and right-hand turns are mirrored. We currently only consider a situation without interaction with other road users. Although the interaction is an important part of driving and inevitably increases discomfort and travel time, we have not observed a significant portion of samples featuring yielding for other road users. To make the optimization study comparable to the naturalistic driving data, we opted to leave the interaction to be investigated in the future. Nevertheless, the negative impact could be mitigated by smart traffic control and cooperative driving methods that reduce potential conflicts [19]. The detailed formulation of the optimization problem is described as follows.

A. Objective function

The optimization minimizes a cost function described by (3), which is simply the weighted sum of travel time T and discomfort D with the weighting factor W is placed on travel time. This allows the scheme to find the comfort-optimal motion by assigning $W = 0$. The weighting can also be interpreted as a measure of the urgency of the trip for the user to choose. It remains an open question though, how to measure passenger comfort in a way that reflects the subjective feeling. We adopted the indicator of discomfort described by (4), which is the integral of squared planar acceleration over time, identical to what was chosen in [14]. Contrary to the use of root-mean-square accelerations, the integral action prevents reducing the discomfort measure by unnecessarily slowing down the vehicle, especially in the

case of $W = 0$. The frequency sensitivity is not considered due to its significantly higher computational demand and the fact that the duration of the maneuver is not sufficiently long to analyze the low-frequency components. Vertical motion is not considered in this study as we assume flat and well-paved road conditions. Improving vertical motion comfort (or ride quality) is more often considered a task for suspension-related studies.

$$J_2 = W \cdot T + D \tag{3}$$

$$D = \int_0^T \left(a_x^2 + a_y^2\right) dt \tag{4}$$

B. Motion definition

The motion of the vehicle is described in the spatial domain as a sequence of waypoints. Each waypoint is defined with respect to a station located on the lane center, containing information about the lateral position and longitudinal velocity. This allows to directly manipulate the vehicle's path and velocity instead of optimizing the input sequence concerning acceleration and steering. The latter is a controller's task instead. The stations are allocated throughout the entire maneuver with an interval of 1 m. At each station, the lateral position is measured locally along the curvature radius (see Fig. 4) and the longitudinal velocity is assumed to be perpendicular to the radius.

The following steps show how the aforementioned objective function can be evaluated using this motion definition. First, the objective function is re-written as (5), since integrating over the entire maneuver is equivalent to summing the integrals between two stations. Combining with the location of the stations, the coordinates of the actual waypoints can be calculated. The heading and curvature at each waypoint can then be approximated by differentiation. The velocity is assumed to vary linearly in time between adjacent waypoints and hence the accelerations are given by (6), where d_k is the interval between two adjacent stations and κ_k is the curvature at waypoint k. The local time variable τ equals zero when the vehicle is at waypoint k, and equals ΔT_k when the vehicle reaches waypoint $k+1$. The latter is the travel time between waypoint k and $k+1$ as given by (7). Finally, the increment of discomfort between the two
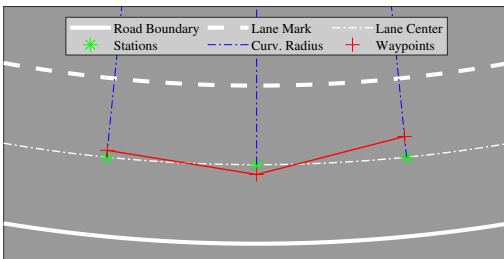

Fig. 4. The definition of the lateral position of waypoints with respect to the stations. A waypoint has a positive lateral position when it is located 90 degrees counter-clockwise from the vehicle's driving direction, irrespective of the direction in which the lane bends.

waypoints is calculated as (8). Thus the value of the cost function can be determined with these equations.

$$J_2 = \sum_{k=1}^{N-1} \left(k\Delta T_k + \Delta D_k\right) \tag{5}$$

$$\begin{aligned} a_{x,k}\left(\tau\right) &= \left(v_{k+1}^2 - v_k^2\right)\big/2d_k \\ a_{y,k}\left(\tau\right) &= \kappa_k\left(v_k + a_{x,k}\tau\right)^2 \end{aligned} \tag{6}$$

$$\Delta T_k = 2d_k\big/\left(v_{k+1} + v_k\right) \tag{7}$$

$$\Delta D_k = \int_{t_k}^{t_k + \Delta T_k} \left(a_{x,k}^2\left(\tau\right) + a_{y,k}^2\left(\tau\right)\right) d\tau \tag{8}$$

C. Scenario and constraints

In this study, we adopt a single-lane roundabout with four connecting arms equally distributed. Standard dimensions recommended for outside built-up areas in the Netherlands are used. Assuming that the vehicle's heading is approximately perpendicular to the curvature radius at each station, the vehicle is considered within the safety corridor as long as the lateral deviation is bounded. Given the lane width of 4.5 m and the fact that most passenger vehicles do not exceed 2 m in width, we consider the maximal deviation of 1 m a sensible choice. The velocity at each station, on the other hand, is bounded according to traffic regulations. The straight segments have an upper limit of $50\,\mathrm{km\,h^{-1}}$, the transition, and the circular section, $30\,\mathrm{km\,h^{-1}}$. The lower bound of velocity is $18\,\mathrm{km\,h^{-1}}$, leading to a lateral acceleration of approximately $1.63\,\mathrm{m\,s^{-2}}$ when driving along the lane center of the circular section. Further lowering this value could contribute to even better comfort but may also harm the intersection's throughput capability and cause danger to other road users. The upper bound of velocity within the intersection is due to safety concerns, while the lower bound eliminates the possibility that the vehicle comes to a full stop to improve comfort in the case of $W = 0$. The chosen lower bound matches the observations from the naturalistic driving data and thus ensures a fair comparison.

D. Initialization and solver

The optimization problem is solved with MATLAB Global Optimization Toolbox. A reasonable motion profile is first generated to initialize the optimization. Intuitively, we set the lateral deviation to all zeros, meaning that the vehicle always follows the lane center. The velocity equals the urban speed limit of $50\,\mathrm{km\,h^{-1}}$ at the start and the end of the maneuver. In between, the velocity gradually reduces to $20\,\mathrm{km\,h^{-1}}$ before the transition and vice versa afterward. From this starting point, a pattern search is performed for a small number of iterations with the objective function evaluated no more than $500 \times N_{\mathrm{var}}$ times, with N_{var} being the number of decision variables. Then the sequential quadratic programming (SQP) method further optimizes the motion profile until convergence. Default settings are used except for the step tolerance being adjusted to 10^{-10} to prevent premature termination.

TABLE I

STATISTICS OF THE FITTED GAMMA DISTRIBUTIONS.

Travel Direction	Acceleration [$\mathrm{m\,s^{-2}}$]	Mode	Mean	SD
Left	Longitudinal	1.25	1.35	0.37
	Lateral	2.82	2.93	0.57
Straight	Longitudinal	0.54	0.82	0.48
	Lateral	1.42	1.55	0.44
Right	Longitudinal	1.15	1.28	0.39
	Lateral	3.62	3.80	0.82

TABLE II

DIFFERENCES BETWEEN PATHS WITH THE SMALLEST AND LARGEST
WEIGHTING ON TRAVEL TIME.

Travel Direction	RMS Diff. [m]	Max Absolute Diff. [m]
Right	0.114	0.370
Straight	0.037	0.099
Left	0.028	0.091

IV. RESULTS

A. Human drivers

The analysis of the naturalistic driving dataset reveals some insights into how human drivers navigate the roundabouts. Fig. 5 is a collection of reconstructed trajectories overlaid on the satellite image of the roundabout. The color variation reflects the change of velocity of the vehicle. The satellite image shows that the horizontal road at this specific location has a wide median. The geometry is optimized to allow the traffic along that direction to pass easily. The effect is evident from the higher average velocity adopted by the corresponding traffic. The vehicles turning into other directions, on the other hand, have to reduce speed to incorporate the larger curvature. The right-turning vehicles approach the minimal distance to the center island in the third quadrant (i.e. the lower-left quarter) and the minimal velocity is obtained in approximately the same location. Driving in this manner reduces the maximum curvature of the path and thus reduces the lateral disturbance on the occupants. The distribution of maximum absolute longitudinal and lateral accelerations are given in Fig. 6. Both variables at each recording location are fit into a Gamma distribution. The statistics of the fitted distribution are given in TABLE I. The figures may not be fully representative due to the incompleteness of the recordings. The traffic vehicles are only detected shortly before the entry. It is likely that the velocity has been adjusted before the recording starts. The same applies to the speed-up phase after leaving the roundabout. This is evident from the fact that the highest recorded velocity is in the range of $8.5\,\mathrm{m\,s^{-1}}$ or $31\,\mathrm{km\,h^{-1}}$, much lower than the speed limit for urban roads.

B. Optimization study

The weighting factor W is influential to the optimal motion profile. The trade-off between comfort and time efficiency is demonstrated by Fig. 7. The sub-figure on the left shows the variation of time and discomfort when W varies between 0 and 4. The values are normalized by dividing by the values corresponding to $W = 0$. When a smaller W is used, the marginal gain of time efficiency is larger than the loss of comfort. The other sub-figure compares the peak accelerations obtained by varying W. The peak lateral acceleration is monotonic increasing with respect to W, which is well anticipated. In contrast, the peak longitudinal acceleration initially decreases with a small W and increases again when $W > 0.5$, depending on the type of the maneuver. This is due to the velocity constraint at the curvy sections. With $W = 0$,

the vehicle slows down quickly to the lowest permissible speed in order to minimize lateral acceleration. With a small W, the cornering velocity is between the lower and upper bounds, requiring less deceleration before the entry. When further increasing W, the vehicle turns at the highest permissible speed and applies the braking later, resulting in a larger longitudinal acceleration. The diamond-shaped markers correspond to the values observed from human drivers. A closer match between the optimized motion and naturalistic driving data is achieved with $W \in [0.5, 1]$.

Besides, we have observed that the spatial paths highly resemble each other despite the variation of W and the corresponding velocity and acceleration profiles. The similarity may suggest a generalizable strategy in utilizing the lane space. The differences in the lateral deviation between using $W = 0$ and $W = 4$ are shown in TABLE II. The optimal motion profiles with $W = 0$ are presented in Fig. 8. In all cases, the optimal motion profiles suggest moving slightly to the left before entering the roundabout, allowing a smaller curvature in that phase. The same is observed when departing the roundabout. In the right-turning case, the optimized path effectively simplifies three consecutive turns (R-L-R) into a single right-hand corner with a small curvature. In the other two cases where the vehicle covers a larger arc angle, the inner part of the circular lane is exploited more. It is intuitive to understand when time efficiency is considered, as a smaller turning radius leads to a shorter distance. For the comfort-optimal case, this could be less intuitive. In the case of steady-state cornering, the smallest possible lateral acceleration is obtained by turning at the lowest permissible velocity and at the largest possible radius. Given an identical linear speed and an identical span angle around the roundabout center, the integral of squared acceleration over time depends linearly on the inverse of radius. It means the smallest D when circulating around the center island is obtained at the largest possible radius, too. However, the benefit of following a small radius lies in the transition phases where the velocity is higher. By allocating space for a smaller curvature where the velocity is higher, the total discomfort may actually be reduced. Therefore, with the current measure of discomfort, driving with a minimal radius inside the roundabout is suggested as the best strategy of space utilization, irrespective of the weight applied to time efficiency.

V. CONCLUSIONS

A. Contributions

In this paper, we investigate the comfort and time efficiency trade-off in motion planning and focus on the compact
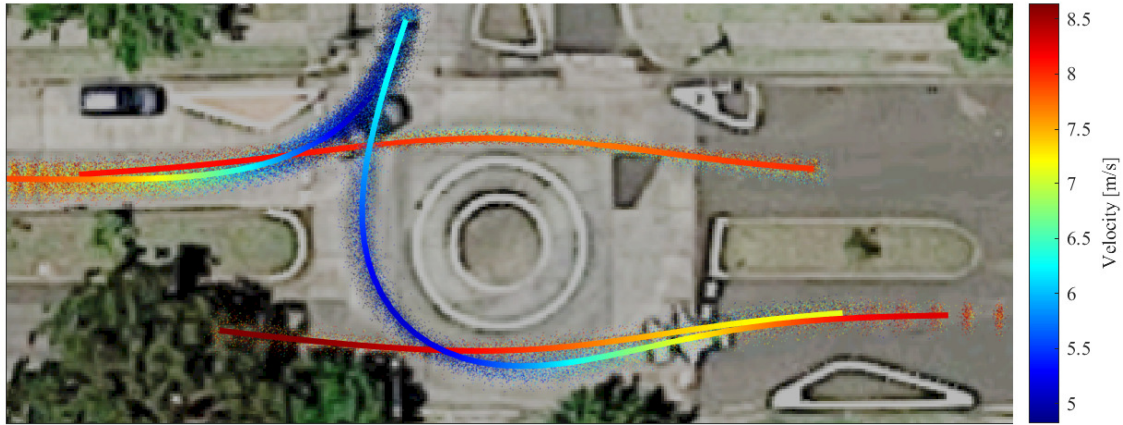
Fig. 5. Naturalistic driving trajectories of human drivers at a roundabout. The velocity is reflected with the color map on the left. The bold lines represent the average trajectories from the same type of maneuver.
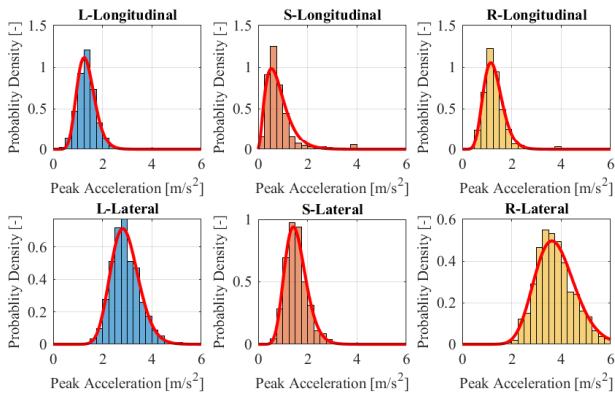

Fig. 6. Distribution of peak longitudinal and lateral accelerations obtained by human drivers at a roundabout. The sample counts on the histograms are normalized to the form of a probability distribution function and the fitted Gamma distribution is described by the red line.
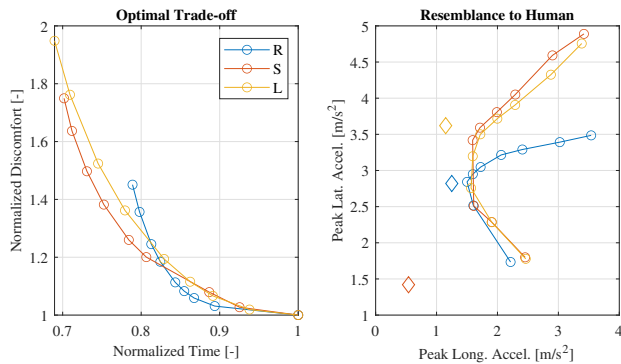

Fig. 7. The influence on optimal motion profiles by varying the weighting factor travel time. The diamond-shaped markers on the right correspond to the values observed from human drivers.
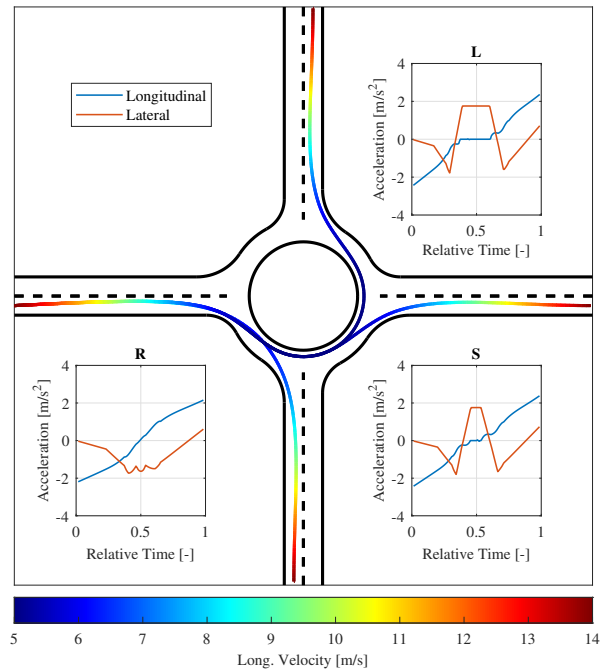

Fig. 8. Comfort-optimal motion profiles at a standard single-lane roundabout.

but comprehensive scenario of a roundabout. We first establish a baseline performance using naturalistic driving data of human drivers, which helps reveal the general acceptance of discomfort. We have processed the original data with significant efforts to overcome the noise and errors. The processed dataset containing smoothed velocity and acceleration information has been made openly accessible via IEEE DataPort. The data suggests that most frequently, the peak acceleration falls between 0.54 and 1.25 m s^{-2} and the lateral acceleration between 1.42 and 3.62 m s^{-2}. The longitudinal acceleration seems lower than expected as the recordings do not cover the major deceleration phases. Lower values

in lateral acceleration are obtained from vehicles driving straight at this roundabout due to the optimized geometry for the traffic in the corresponding direction. Next, a numerical optimization study is performed, where the objective is to minimize the weighted sum of discomfort and travel time. The comfort-optimal motion profiles are found by assigning $W = 0$, aiming to benefit the passengers susceptible to motion sickness. With $W \in [0.5, 1]$, human-like magnitudes of lateral acceleration are obtained. Further increasing the weight on time efficiency would result in quick degradation of comfort and a higher velocity within the intersection. The optimization study also shows that the manner of space utilization is similar between different weighting choices. The major difference comes from the velocity profile instead. The path optimization part remains non-trivial and further investigation is still required.

B. Limitations and Future Works

This study mainly focused on the roundabout scenario, which is sufficiently complex for human drivers and motion planning algorithms but nevertheless not fully representative of the daily use of a passenger vehicle. A more comprehensive testing scenario needs to be developed in order to examine the benefits of comfort-oriented motion planning algorithms. The roundabout used in the optimization study is also in a simple form. Extensions to more complex road types, e.g., multi-lane or turbo roundabouts, highway ramps, etc., could be interesting to study in the future. As indicated previously, the incomplete recordings in the naturalistic driving dataset prevent us from fairly evaluating the time efficiency of human drivers. Thus some doubts remain on the observed distribution of the longitudinal acceleration and the performance gain of the optimization study cannot be properly demonstrated as a consequence. This could be resolved by using alternative data sources, e.g., drones or onboard measurements, that do not have the occlusion problem. Additionally, the interaction with other road users is not considered in this study. In practice, the optimization scheme is capable of handling this by, for example, constraining the velocity at the entry point to zero or constraining the moment of entry. The results found with our optimization study may still be further exploited for developing path generation methods or adopted as template motion profiles. The similarity in the optimal paths should also be studied in order to determine the performance loss by adopting a decoupled approach of path and velocity planning for comfort and time efficiency. To validate the findings of the optimization study, it is highly beneficial to observe in experiments whether the quantitative comfort measure correlates with the occupants' subjective comfort, and whether the improvements can be reflected on the their task performance.

References

[1] Panagiotis Matsangas, Michael E McCauley, and William Becker. The effect of mild motion sickness and sopite syndrome on multitasking cognitive performance. *Human factors*, 56(6):1124–1135, 2014.

[2] Monica LH Jones, Victor C Le, Sheila M Ebert, Kathleen H Sienko, Matthew P Reed, and James R Sayer. Motion sickness in passenger vehicles during test track operations. *Ergonomics*, 62(10):1357–1371, 2019.

[3] Tugrul Irmak, Daan M Pool, and Riender Happee. Objective and subjective responses to motion sickness: the group and the individual. *Experimental Brain Research*, 239(2):515–531, 2021.

[4] Eike A Schmidt, Ouren X Kuiper, Stefan Wolter, Cyriel Diels, and Jelte E Bos. An international survey on the incidence and modulating factors of carsickness. *Transportation research part F: traffic psychology and behaviour*, 71:76–87, 2020.

[5] Jean-Paul Laumond et al. *Robot motion planning and control*, volume 229. Springer, 1998.

[6] David González, Joshué Pérez, Vicente Milanés, and Fawzi Nashashibi. A review of motion planning techniques for automated vehicles. *IEEE Transactions on Intelligent Transportation Systems*, 17(4):1135–1145, 2015.

[7] Ray Lattarulo, Enrique Martí, Mauricio Marcano, Jose Matute, and Joshue Pérez. A speed planner approach based on bézier curves using vehicle dynamic constrains and passengers comfort. In *2018 IEEE International Symposium on Circuits and Systems (ISCAS)*, pages 1–5. IEEE, 2018.

[8] Yuchuan Du, Chenglong Liu, and Yishun Li. Velocity control strategies to improve automated vehicle driving comfort. *IEEE Intelligent transportation systems magazine*, 10(1):8–18, 2018.

[9] Ioannis A Ntousakis, Ioannis K Nikolos, and Markos Papageorgiou. Optimal vehicle trajectory planning in the context of cooperative merging on highways. *Transportation research part C: emerging technologies*, 71:464–488, 2016.

[10] Cesare Certosini, Renzo Capitani, and Claudio Annicchiarico. Optimal speed profile on a given road for motion sickness reduction. *arXiv preprint arXiv:2010.05701*, 2020.

[11] Antonio Artuñedo, Jorge Villagra, and Jorge Godoy. Jerk-limited time-optimal speed planning for arbitrary paths. *IEEE Transactions on Intelligent Transportation Systems*, 2021.

[12] Antonio Artuñedo, Jorge Godoy, and Jorge Villagra. Smooth path planning for urban autonomous driving using openstreetmaps. In *2017 IEEE Intelligent Vehicles Symposium (IV)*, pages 837–842. IEEE, 2017.

[13] Marlies Mischinger, Martin Rudigier, Peter Wimmer, and Andreas Kerschbaumer. Towards comfort-optimal trajectory planning and control. *Vehicle System Dynamics*, 2018.

[14] Heechan Shin, Donghyuk Kim, and Sung-Eui Yoon. Kinodynamic comfort trajectory planning for car-like robots. In *2018 IEEE/RSJ International Conference on Intelligent Robots and Systems (IROS)*, pages 6532–6539. IEEE, 2018.

[15] Zaw Htike, Georgios Papaioannou, Efstathios Siampis, Efstathios Velenis, and Stefano Longo. Minimisation of motion sickness in autonomous vehicles. In *2020 IEEE Intelligent Vehicles Symposium (IV)*, pages 1135–1140. IEEE.

[16] Aleksandra Deluka Tibljaš, Tullio Giuffrè, Sanja Surdonja, and Salvatore Trubia. Introduction of autonomous vehicles: Roundabouts design and safety performance evaluation. *Sustainability*, 10(4):1060, 2018.

[17] Yuxiang Zhang, Bingzhao Gao, Lulu Guo, Hongyan Guo, and Hong Chen. Adaptive decision-making for automated vehicles under roundabout scenarios using optimization embedded reinforcement learning. *IEEE Transactions on Neural Networks and Learning Systems*, 2020.

[18] Alex Zyner, Stewart Worrall, and Eduardo M Nebot. Acfr five roundabouts dataset: Naturalistic driving at unsignalized intersections. *IEEE Intelligent Transportation Systems Magazine*, 11(4):8–18, 2019.

[19] Peng Hang, Chao Huang, Zhongxu Hu, Yang Xing, and Chen Lv. Decision making of connected automated vehicles at an unsignalized roundabout considering personalized driving behaviours. *IEEE Transactions on Vehicular Technology*, 2021.